Automatic parcellation of human cortical gyri and sulci using standard anatomical nomenclature

Christophe DESTRIEUX, MD[a,b,c,d,*], **Bruce FISCHL, PhD**[e,f], **Anders DALE, PhD**[g], and **Eric HALGREN, PhD**[g]

[a] UMRS Inserm U930, CNRS ERL 3106, Université François Rabelais de Tours, Tours, France

[b] Université François Rabelais de Tours, Faculté de Médecine, Tours, France

[c] CHRU de Tours, Tours, France

[d] IFR 135 « Imagerie fonctionnelle », Tours, France

[e] Athinoula A. Martinos Center for Biomedical Imaging, NMR Center, Harvard Medical School, Charlestown, MA, USA

[f] Computer Science and AI Lab/HST, Mass. Institute of Technology, Cambridge, MA, USA

[g] University of California San Diego, Departments of Radiology and Neurosciences, La Jolla, CA, USA

Abstract

Precise localization of sulco-gyral structures of the human cerebral cortex is important for the interpretation of morpho-functional data, but requires anatomical expertise and is time consuming because of the brain s geometric complexity. Software developed to automatically identify sulco-gyral structures has improved substantially as a result of techniques providing topologically-correct reconstructions permitting inflated views of the human brain. Here we describe a complete parcellation of the cortical surface using standard internationally-accepted nomenclature and criteria. This parcellation is available in the FreeSurfer package. First, a computer-assisted hand parcellation classified each vertex as sulcal or gyral, and these were then subparcellated into 74 labels per hemisphere. Twelve datasets were used to develop rules and algorithms (reported here) that produced labels consistent with anatomical rules as well as automated computational parcellation. The final parcellation was used to build an atlas for automatically labeling the whole cerebral cortex. This atlas was used to label an additional 12 datasets, which were found to have good concordance with manual labels. This paper presents a precisely-defined method for automatically labeling the cortical surface in standard terminology.

Precise description of the gross anatomy of the cerebral cortex only appeared in the second third of the 19th century for at least two reasons. Initially, its complex tridimensional

*Corresponding author: Christophe DESTRIEUX, Laboratoire d Anatomie, Faculté de Médecine, 10 Bd Tonnellé, 37032 Tours, France, tel: (33) 2 47 36 61 36 – fax: (33) 2 47 36 62 07, destrieux@med.univ-tours.fr.

anatomy made the cortex difficult to systematically describe and represent, especially at a time when no preservation method was available. Although the great 16th century anatomist Andreas Vesalius was able to describe the human body in great detail (Vesale, 2008), he surprisingly only wrote a few lines about the cortex and rejected any clear organization for this part of the brain (Vesalius, 1543), describing gyri as "clouds painted by children in school", and citing Erasistrate who depicted them as "intestinal loops". Vesalius denied that the cerebral cortex has any role in "intelligence," and, thus, neglected to precisely describe it. This lack of interest for cortical anatomy remained until Gall developed his theory of localized cerebral organs, each of them being specialized in a precise field (Gall, 1807). Although this conception was closer to dogma than to a scientific theory, it opened the way to localisationism and, consequently, the need for a precise description of the brain, especially its cortex.

During the second third of the 19th century, multiple attempts were made to precisely describe the sulco-gyral pattern of the brain. For instance, Leuret and Gratiolet (Leuret and Gratiolet, 1839), Gratiolet (Gratiolet, 1854), and a few years later, Ecker (Ecker, 1873), and Broca (Broca, 1877, 1878) proposed more or less precise rules for identifying the gyri and sulci of the human cerebral cortex. Finally, at the end of the 19th century, several names proposed by these authors and others, came to be consistently used for the corresponding sulcus or gyrus. In the same time, the anatomical community tried to unambiguously associate a single name to each structure of the human body leading to the first anatomical nomenclature, the Basle Nomina Anatomica, published in 1895 ((Kachlik et al., 2008; Whitmore, 1999). After several revisions, the actual nomenclature, the Terminologia Anatomica (TA) was published in 1998 (Federative Committee on Anatomical Terminology, 1998). This database lists the Latin anatomical names and the English translation of 7444 anatomical structures for the gross anatomy of the entire human body. Nevertheless, the terms included in this reference are insufficient for precise description of the cerebral cortex. For example, only 4 terms are included for the lateral aspect of the occipital lobe (occipital pole, sulcus lunatus, preoccipital notch, and transverse occipital sulcus), obviously too few to adequately describe this region. Moreover, the TA just lists the names of cortical structures without any precise definition.

Alternative parcellation schemes have been proposed that more or less follow the TA (Caviness et al., 1996; Duvernoy et al., 1991; Ono et al., 1990). This state of affairs can be highly confusing, since anatomical description is a matter of convention: depending on the chosen number of parcellation units, and of their respective limits, several parcellation schemes may be defined, and the same anatomical label may correspond to a parcellation unit whose boundaries vary in different conventions. A pervasive issue is how far gyral labels extend into the bounding sulci. For example, the precentral gyrus maybe considered (1) as the part of the cortex located between the fundus of the precentral sulcus anteriorly, and the fundus of the central sulcus posteriorly, or (2) restricted to the cortex located between the posterior bank of the precentral sulcus, and the anterior bank of the central sulcus. Even if the same parcellation scheme is used, the definition of the different parcellation units is not always precise enough to ensure good reproducibility between observers. In some cases this is due to a lack of precise anatomical boundaries between contiguous cortical structures: for instance, the boundaries of the temporal pole or of the occipital lobe are unclear, usually not precisely defined in the literature, and may thus vary from observer to observer. Moreover, this complex sulco-gyral organization varies across individuals (Ono et al., 1990; Zilles et al., 1997), making its manual description and correspondence across different brains difficult and often unreliable. As a consequence, manual identification of sulco-gyral structures, for instance from Magnetic Resonance Imaging (MRI), is difficult to perform for the whole cortex, time consuming, requires a high level of anatomical expertise, and a precise definition of the rules used for this parcellation.

Fortunately, underlying this complex 3D architecture is a simple topology: the cortex is a continuous neuronal sheet that more or less complexly folds during embryonic life. Methods have been developed to reconstruct precise and topologically correct representations of the cortical surface from structural MRI (Dale et al., 1999; Dale and Sereno, 1993; Fischl et al., 1999a; Van Essen and Drury, 1997). These representations can be unfolded, allowing the consistent deep sulcal pattern to be visualized, in contrast to the unfolded brain where the highly variable surface folds visually predominate. Due to the sheet-like topology of the cortex, surface based coordinate systems (Fischl et al., 1999a; Fischl et al., 1999b; Thompson et al., 2000; Van Essen et al., 1998) may be more appropriate for the anatomy of the brain than classical volume based coordinate systems (Talairach and Tournoux, 1988): they provide better inter-subject averaging and allow the development of tools for automatically parcellating the cortex in a reproducible and accurate way (Desikan et al., 2006; Fischl et al., 2004).

This paper describes the sulco-gyral parcellation used to build a surface based atlas (Fischl et al., 2004) included in the FreeSurfer package (http://surfer.nmr.mgh.harvard.edu/). Rather than provide a novel nomenclature or parcellation of the cortex, we have attempted to follow widely accepted anatomical conventions, and thus encourage its adoption by the imaging community.

We first unambiguously labeled every point of the cerebral cortex in a group of healthy subjects (*Initial set*) by defining precise anatomical rules. These rules were adapted from a classical anatomical nomenclature (Duvernoy et al., 1991) relatively close to the TA, but defining structures in a more precise way than this official nomenclature. We then apply these rules to manually label the cerebral cortex in 12 different healthy subjects, thus creating a *Training set* for an automated labeling procedure. The resulting parcellations were examined to reveal areas where the automated labels were unreliable. The algorithms used for manual labeling were then changed to increase reliability, or if this was not possible, areas were amalgamated to arrive at units that could be consistently parcellated. We describe here this process, as well as the detailed final algorithms for manually-labeling the cortical gyri and sulci. Here (and in the supplemental online material), cortical parcellations are displayed for twelve healthy individuals.

1 Materials and method

1.1 Nomenclature of individual brains

1.1.1 Subjects – Scanning procedure—Twenty-four healthy right-handed volunteers were included in this study: 12 male (aged 18–25 years, mean 21.67 year) and 12 female (21–33 year-old, mean 25.33 years). They were scanned on a 1.5 T Siemens Sonata scanner. Two high-resolution whole-head T1 weighted MPRAGE scans were collected: TR=2730 ms, TE = 3.39 ms, Flip angle = 7°, slice thickness = 1.3 mm, 128 slices, FOV = 256mm x 256mm, matrix = 256×256). These parameters were empirically optimized for contrast between gray matter, white matter and cerebrospinal fluid (CSF). The two scans were motion-corrected and averaged to increase the signal to noise ratio (SNR). Two groups of 12 subjects (6 male and 6 female) were defined, the first (*Initial set*) was used to develop and test the anatomical rules included in this paper, while the second (*Training set*) was used to train the automated labeling software.

1.1.2 Reconstruction process—The detailed reconstruction process of the cortical surface has been previously described (Dale et al., 1999; Fischl et al., 1999a): after correction for intensity variations due to magnetic field inhomogeneities, non-brain tissues were removed from the T1 normalized images using a hybrid watershed/surface deformation procedure (Segonne et al., 2004). The brain was segmented using the signal intensity and

geometric structure of the gray-white interface. Each hemisphere was automatically disconnected from the other and from the mesencephalon, resulting in two binarized white matter volumes. The surface of each white matter volume was tessellated with a triangular mesh, and deformed to obtain a smooth and accurate representation of the gray-white interface. After the topology of this surface was automatically corrected (Segonne et al., 2007), it was inflated in a way that retains much of the shape and metric properties of the original gray-white interface. This process unfolded sulci of the cortex, leading to a representation where the whole cortical surface (i.e. sulcal and gyral) was visible. During this process, the vertices that lie in concave region moved outwards while the vertices in convex regions moved inwards. The average convexity ("sulc" maps in FreeSurfer) evaluates this movement for each point of the cortical surface, and was color encoded to depict the large sulci and gyri. Large sulci (for instance the lateral sulcus) or gyri sometimes contained smaller structures (for instance short and long insular gyri and central sulcus of the insula) for which the average convexity was very similar. Another parameter, the mean curvature, ("curv" maps in FreeSurfer) was more efficient to describe these secondary and tertiary folding patterns. At the end of the reconstruction process, several views were available for each hemisphere depending on the extent of the cortical inflation and the surface that was used: pial (no inflation, gray-CSF interface), white (no inflation, gray-white interface), inflated (inflation, gray-white interface).

1.1.3 Parcellation scheme—The nomenclature used in this study is mainly based on that of Duvernoy (Duvernoy et al., 1991). First, a name database was created to list the anatomical terms used in this book and their corresponding definitions. For each of the sulcal and gyral structures that were listed per hemisphere, the database contained: the lobe(s) and aspect(s) of the hemisphere this structure pertains to, its limits to contiguous cortical structures, and alternative names found in the literature (Ono et al., 1990).

Based on this name database, the entire cortex was divided into sulcal and gyral cortices depending upon the values of local mean curvature and average convexity obtained from the reconstructed cortical surfaces output from FreeSurfer (Supplementary material, supp-Fig 1). For most of the structures, the limit was given by the average convexity value: vertices with an average convexity value below a given threshold were considered sulcal, and vertices with value equal or above this threshold were considered gyral. This threshold was empirically chosen to set the sulco-gyral limit close to the junction point between the brain convexity and the outer part of sulcal banks on the pial views and T1 images. This value equaled zero for most of the structures located at the lateral and inferior aspects of the brain. A value of 0.18 was chosen for most of the structures located at the medial aspect of the hemisphere. Since the insula is situated deep in the lateral sulcus, the average convexity value was negative for each vertex in this region and therefore does not distinguish gyral from sulcal cortex of the insular lobe and opercula. In these regions, the mean curvature was used in a similar way: vertices with a positive mean curvature value were considered sulcal, and vertices with non-positive values were considered gyral.

Once the whole cortical surface was classified as gyral or sulcal, limits between contiguous sulci and gyri were directly drawn by hand on the inflated surface using tools included in the FreeSurfer package (Supplementary material, supp-Fig 2). The location of these limits was defined by the nomenclature rules previously defined in the name database. Once a cortical structure (gyral or sulcal) was bounded by these lines and the sulco-gyral limits, it was associated to a label chosen in the name database. For a few large structures, an additional sub-parcellation was used. For instance the cingulate gyrus was subdivided on based on estimated cytoarchitectonic and functional criteria as proposed by Vogt (Vogt et al., 2003; Vogt et al., 2006). Details of these additional parcellations are directly provided in the results section. Using this process, each vertex of the cortical surface was assigned to an

anatomical label from the name database. On the midline an area labeled Medial_wall grouped structures not involved by the inflation process, including the hippocampus, thalamus, ventricles, and corpus callosum. This Medial_wall parcellation was not considered in the quantification of concordance index, area, etc., presented below.

1.1.4 Improvement of anatomical rules—The first set of 12 subjects (*Initial set*) was used to test and improve the nomenclature rules defined in the name database (Destrieux et al., 1998). The inflated cortical surface was labeled by one of the authors (CD), some of the anatomical rules previously defined were modified, and a labeling procedure was defined. Since manual nomenclature of a cortical structure depends on the labels attached to the surrounding structures, the labeling procedure also included the order to be followed to perform the cortical parcellation.

1.1.5 Creation of the database—The resulting name database and procedure were used to label the second set (*Training set*) of subjects. After these 12 independent subjects (24 hemispheres) were labeled, the dataset was visually inspected for errors resulting in mislabeling of large cortical regions: the 12 brains were registered to Talairach space (Talairach and Tournoux, 1988), snapshots of the labeled surfaces were visually compared, and errors were corrected.

1.2 Automated labeling

1.2.1 Probabilistic labeling—The manually labeled second set of hemispheres was used as a *Training set* to build a statistical surface-based atlas in order to automatically label "new" hemispheres (Fischl et al., 2004). The labeling procedure was modeled as a first order anisotropic non-stationary Markov random field on the labels of the cortical surface that captured the spatial relationships and variance between the labels defined in the training set. The probability of a label at a certain vertex is based on a number of pieces of information, including the curvature and average convexity of the cortical surface, prior labeling probability for that vertex, as well as the labels of vertices in a local neighborhood. See (Fischl et al., 2002; Fischl et al., 2004) for a detailed derivation of the procedure.

1.2.2 Concordance of auto/manual labelling—The automated and manual labeling for the *Training set* were compared using a Jackknife/leave-one-out procedure (Fischl et al., 2004): for each of the 12 *Training* subjects, an atlas was built with the remaining 11 and was used to automatically label the excluded subject.

Three cortical surface area measures were computed for each of the defined parcellation units: the area derived from the manual labeling ($Area_{manu}$), from the automated labeling ($Area_{auto}$), and the area of vertices commonly labeled by the manual and automated procedure ($Area_{common}$). A concordance index (CI) was computed for each of the defined parcellation units as a DICE coefficient corresponding to the area of vertices labeled the same by both procedures, divided by the average area of this parcellation unit obtained by automated and manual procedure: $CI = 2.Area_{common}/(Area_{manu} + Area_{auto})$. It theoretically varied from 0 (no concordance at all) to 1 (perfect concordance between automated and manual procedures). Similarly, a global CI was computed for each hemisphere by pooling results for the whole cortex.

To take in account boundary effects (see discussion section), CIs were computed for the whole cortical surface, but also separately for the boundary and core vertices. The boundary vertices were defined as vertices having at least one neighbor vertex differently labeled (Supplementary material, supp-Fig 1). Conversely, core vertices were defined as labeled the same as all their neighbors. $CI_{original}$ (CI_o) and $CI_{boundarycorrected}$ (CI_c) were respectively

defined as CI computed without and after this boundary correction. Finally, the percentage of hidden cortex, including sulcal cortex and lateral fossa, was computed for each hemisphere.

1.2.3 Improvement of the parcellation—Parcellation units with reproducibly low CI_C across subjects of the *Training set* were inspected: some parcellations that were very small, difficult to localize even by a trained anatomist, or very variable were grouped with a larger neighboring parcellation unit (for instance, anterior and posterior subcentral sulci were grouped with the subcentral gyrus). 9 groups of structures were created (see table 1, indices 1–8 and 17) and finally, each hemisphere was segmented into 74 different sulco-gyral cortical units.

2 Results

We here present the final improved parcellation (table 1) used to manually label the *Training set* used by the automated labeling procedure distributed with the FreeSurfer package since August 2009 (Freesurfer v4.5, aparc.a2009s/Destrieux.simple.2009-07-29.gcs atlas). In the text, the common name of each parcellation unit was ***bold italic type***, alternative anatomical names found in the literature were given in parentheses (), and were followed in square brackets [] by the label used in the FreeSurfer interface, and by an arbitrary index used in tables and figures.

Despite its small size (12 subjects), important variations of the sulco-gyral pattern observed in the *Training set* were described and their frequencies were given for right (R) and left (L) hemispheres. As an example, the parcellation scheme is provided in inflated (fig. 1) and pial (fig. 2) views for a left hemisphere of one subject. The parcellations for both hemispheres of the 12 included individuals are provided in inflated and pial views as supplementary online material (supp-Fig 3 to 6).

The cortical surface was divided in frontal, temporal, parietal, occipital, insular and limbic lobes.

2.1 Frontal Lobe

The frontal lobe is the largest division, forming the anterior part of the lateral, medial and ventral aspects of the brain.

2.1.1 Limits of the frontal lobe—*At the lateral aspect* of the brain, the frontal lobe is limited from the more posterior parietal lobe by the central sulcus and from the inferiorly located insula by the superior and anterior parts of the circular sulcus of the insula (see bellow: insular lobe). The ***central sulcus*** (Rolando's fissure) [S_central, 45] originates at the superior edge of the hemisphere, courses antero-inferiorly, and ends close to the superior part of the circular sulcus of the insula.

The medial aspect of the frontal lobe is inferiorly bounded by the ***cingulate sulcus***: the main part of this sulcus parallels the anterior and middle parts of the corpus callosum and limits the medial aspect of the frontal lobe from the cingulate gyrus. Similarly to the nomenclature we adopted for the neighboring parts of the cingulate gyrus, it was subdivided in: ***anterior, middle-anterior and middle posterior parts*** (see bellow, limbic lobe, for a detailed description). The latter is continued caudally by the ***marginal part of the cingulate sulcus*** [S_cingul-Marginalis, 46] that ascends up to the dorsal edge of the hemisphere between the frontal and parietal lobes, and ends just posterior and medial to the superior tip of the central sulcus.

2.1.2 Main Frontal sulci and gyri

2.1.2.1 *Lateral aspect* **of the frontal lobe:** The *precentral sulcus* anteriorly parallels the central sulcus and is divided into superior [S_precentral-sup-part, 69] and inferior parts [S_precentral-inf-part, 68], connected at right angles, respectively to the superior and inferior frontal sulci. The limits between precentral, superior and inferior frontal sulci were drawn on the "white" reconstructed surface at the point were the change in sulcal direction was obvious. If both segments of the precentral sulcus were continuous (R: 1/12; L: 2/12), a limit was arbitrarily drawn at its midpoint. Conversely, if a large third segment was present (R: 0; L: 1/12), it was arbitrary split in two parts respectively grouped with the superior and inferior parts of precentral sulcus.

The *precentral gyrus* [G_precentral, 29] is located between the central and precentral sulci. A virtual line, anteriorly limiting the precentral gyrus, joined the inferior tip of the superior segment of the precentral sulcus, to the superior tip of its inferior segment. The pre and postcentral gyri are connected together by two *plis de passage*: the subcentral and paracentral gyri (see bellow: fronto-parietal *plis de passage*). Only the *subcentral gyrus* (or central operculum), limited by the anterior and posterior subcentral sulci [G_and_S_subcentral, 4] is located at the lateral aspect of the hemisphere where it turns around the inferior tip of the central sulcus. The limit between the precentral and subcentral gyri was defined as the straight line drawn on the inflated view between the inferior tips of the central and precentral sulci.

The *inferior frontal sulcus* [S_front_inf, 52] is connected to the inferior part of the precentral sulcus and runs parallel to the superior segment of the circular sulcus of the insula. It appeared discontinuous on the inflated view and didn't reach the frontal pole but was often (R: 7/12; L: 3/12) anteriorly connected to the lateral orbital sulcus that seemed to inferiorly continue its course. For this reason, precise delineation of the limit between inferior frontal and lateral orbital sulci was sometimes problematic

The *inferior frontal gyrus* (or F3) is located between the circular sulcus of the insula, and the inferior frontal sulcus continued by the lateral orbital sulcus. Its posterior limit was defined as the line joining the inferior tip of the precentral sulcus, the anterior subcentral sulcus, and the neighboring superior part of the circular sulcus of the insula. The inferior frontal gyrus is divided in 3 parts by the *horizontal and vertical rami of the anterior part of the lateral sulcus*. These 2 small rami originate close to the junction of the anterior and superior segments of the circular sulcus of the insula and run within the inferior frontal gyrus. The horizontal ramus of the lateral sulcus [Lat_Fis-ant-Horizont, 39] was nearly always connected to the superior segment of the circular sulcus of the insula that it continued anteriorly (R: 12/12; L: 11/12). On the inflated view, the vertical ramus of the lateral sulcus [Lat_Fis-ant-Vertical, 40] appeared connected to the superior segment of the circular sulcus of the insula in only 2 thirds of the hemispheres (R: 8/12; L: 7/12). In the remaining hemispheres, this sulcus had a similar ascending course in the inferior frontal gyrus, but was disconnected from other sulcal structures. On the inflated view, a straight line was drawn to virtually continue the ascending direction of the vertical ramus of the lateral sulcus, up to the inferior frontal sulcus. Similarly, a horizontal line anteriorly extended the horizontal ramus of the lateral sulcus towards the inferior frontal sulcus in about half of the hemispheres (R: 7/12; L: 5/12), and towards the lateral orbital sulcus in other cases. The *triangular part of the inferior frontal gyrus* [G_front_inf-Triangul, 14] is located between these two lines. The *opercular part of the inferior frontal gyrus* [G_front_inf-Opercular, 12] is posterior to the vertical ramus/line, whereas its *orbital part* [G_front_inf-Orbital, 13] is antero-inferior to the horizontal ramus/line. At the basal aspect of the frontal lobe (see bellow), the orbital part is medially and inferiorly continued by the orbital gyri from which it is limited by the *lateral orbital sulcus* [S_orbital_lateral, 62]. When the latter was short, the

limit between the lateral and basal aspects of the frontal lobe was unclear and was only defined by the line that continued the lateral orbital sulcus on the "pial" view. The posterior limit of the orbital part is the anterior segment of the circular sulcus of the insula. The inconstant *triangular sulcus* and *sulcus diagonalis* arise from the inferior frontal sulcus. They respectively run towards the triangular and opercular parts of the inferior frontal gyrus. Due to their variability, these 2 sulci were included for labeling into the inferior frontal sulcus which they originated from.

The *superior frontal sulcus* [S_front_sup, 54] is a long, often discontinuous sulcus running parallel to the superior edge of the hemisphere, from the superior part of the precentral sulcus towards the frontal pole that it doesn't reach, being interrupted by the transverse frontopolar gyri and sulci (see bellow).

The *middle frontal gyrus* (or F2) [G_front_middle, 15] is limited: superiorly by the line joining the segments of the superior frontal sulcus and the transverse frontopolar sulcus, inferiorly by the inferior frontal and lateral orbital sulci, posteriorly by both segments of the precentral sulcus and by the line joining them. The anterior limit of the middle frontal gyrus is formed by the transverse frontopolar sulcus, the frontomarginalis sulcus, and the line joining: the lateral tip of the frontomarginalis sulcus, the anterior tip of the lateral orbital sulcus, and the anterior tip of the inferior frontal sulcus. A discontinuous *middle frontal sulcus* [S_front_middle, 53] was usually present (R: 12/12; L: 11/12) within the middle frontal gyrus. Its length is variable but it is more anterior than the superior and inferior frontal sulci and reaches the frontal pole, whereas it is not connected to the precentral sulcus. It is independent or connected to the superior or inferior frontal sulci, from which it is sometimes difficult to distinguish.

2.1.2.2 Medial aspect of the frontal lobe: The **superior frontal gyrus** (or F1) [G_front_sup, 16] forms the supero-medial edge of the hemisphere and is thus visible on both lateral and medial views. It was infero-laterally limited by the line joining: the segments of the superior frontal sulcus, the medial tips of the transverse frontopolar and frontomarginalis sulci; posteriorly by the line joining: the superior tip of the precentral sulcus, the paracentral sulcus, and the cingulate sulcus; infero-medially by the marginal and main parts of the cingulate sulcus; and antero-inferiorly by the line joining the medial tip of the frontomarginal sulcus to the anterior tip of the *suborbital sulcus*. This *suborbital sulcus* (or sulcus rostrales or supraorbital sulcus) [S_suborbital, 70] is a small sulcus parallel to the anterior part of the cingulate sulcus, running towards the frontal pole. It is sometimes paralleled by an inconstant smaller dorsal groove that may be called *superior* suborbital sulcus. Nevertheless, this *superior* suborbital sulcus was included in the label [G_and_S_cingul-Ant, 6] because of its inconsistency and since it was difficult to distinguish from a ramus of the cingulate sulcus on the inflated views.

The *gyrus rectus* or straight gyrus [G_rectus, 31] is at the junction between the medial and inferior aspects of the frontal lobe: it is located between the suborbital sulcus supero-medially, and the medial orbital sulcus laterally, the latter being extended on the reconstructed pial surface by a straight line joining its anterior tip to the frontal pole.

2.1.2.3 Frontal pole: The clear organization of the frontal lobe into superior, middle and inferior frontal gyri is lost at the frontal pole since these gyri are interrupted by several transverse gyri and sulci, comprising from superior to inferior: transverse frontopolar sulcus and gyrus, fronto-marginal sulcus and gyrus. The *fronto-marginal sulcus* (sulcus of Wernicke) runs parallel to the junction between the lateral and ventral aspects of the frontal lobe. It was sometimes connected to one of the neighboring sulci: middle (R: 5/12; L: 4/12) or superior frontal sulcus (R: 0/12; L: 2/12). The *fronto-marginal gyrus* is located just

inferior to this sulcus and is continuous with the orbital gyri. We defined the limit between these 2 gyri on the reconstructed pial surface, as the edge between the lateral and ventral aspects of the frontal lobe. The frontomarginal sulcus and gyrus were grouped in the same label: [G_and_S_frontomargin, 1]. One (R: 7/12; L: 12/12) or two (R: 5/12; L: 0/12) *transverse frontopolar sulci* also ran perpendicular to the superior frontal sulcus and were accompanied by small depressions on the cortical surface that were only visible on the pial view. The *transverse frontopolar gyrus or gyri* are located between the transverse frontopolar sulci superiorly, and the fronto-marginal sulcus inferiorly. Since they have no other sulcal border, we had to define 2 additional arbitrary limits; laterally, a line joining the lateral tips of the transverse frontopolar and fronto-marginal sulci limited the transverse frontopolar gyrus or gyri. Medially, they were limited by the supero-medial edge of the frontal lobe. Due to this high variability (number and presence or absence of accessory cortical depressions), the transverse frontopolar sulci and gyri were included in the same label [G_and_S_transv_frontopol, 5].

2.1.2.4 Ventral aspect of the frontal lobe: Since the ventral aspect of the frontal lobe (or orbital lobe) is continuous with several surrounding structures we had to define its limits by drawing a line made of several segments on the reconstructed pial surface. The first segment joined the anterior part of the circular sulcus of the insula to the posterior tip of the lateral orbital sulcus. It limited the ventral aspect of the frontal lobe from the orbital part of the inferior frontal gyrus. It was continued by a second segment, drawn on the reconstructed pial view, which began from the lateral orbital sulcus, and ran along the infero-lateral edge of the hemisphere towards the midline. This segment limited the ventral aspect of the frontal lobe from the middle frontal and frontomarginal gyri located above. The medial limit of the ventral aspect of the frontal lobe is clearly limited from the gyrus rectus by the *medial orbital sulcus* [S_orbital_med-olfact, 63], which runs parallel to the infero-medial edge of the frontal lobe. The medial orbital sulcus is also named the olfactory sulcus, since it is located just superior to the olfactory bulb and tract. Finally, the last segment posteriorly limiting the inferior aspect of the frontal lobe, joined the posterior tip of the medial orbital sulcus to the inferior tip of the anterior segment of the circular sulcus of the insula.

The ventral aspect of the frontal lobe is made of 4 orbital gyri (anterior, posterior, lateral and medial) limited by the *H-shaped orbital sulcus*. Although this sulcus is commonly described as 2 longitudinal rami linked by a transverse one, we failed to find a consistent organization, and so it was labeled as a whole [S_orbital-H_shaped, 64]. Similarly, the 4 *orbital gyri* were grouped in a single label [G_orbital, 24].

2.2 Insula

Since the insula is deeply located its average convexity value was negative and fine sulco-gyral organization of this area was only visible using the mean local curvature maps. On the inflated view, the insula is clearly limited by the **circular sulcus of the insula** divided in 3 segments: *superior* [S_circular_insula_sup, 49], horizontally limiting the insula from the subcentral and inferior frontal gyri; *anterior* [S_circular_insula_ant, 47], vertically limiting the insula from the orbital gyri; and *inferior* [S_circular_insula_inf, 48], obliquely limiting the insula from the superior aspect of the superior temporal gyrus. The *lateral sulcus or fissure* results from the juxtaposition of fronto-parietal and temporal opercula, and is classically divided in anterior, middle and posterior segments (Duvernoy et al., 1991). The superior and anterior segments of the circular sulcus of the insula anteriorly fuse to form the *anterior segment of lateral sulcus* that rapidly splits into *vertical* [Lat_Fis-ant-Vertical, 40] *and horizontal rami* [Lat_Fis-ant-Horizont, 39]. Since the inflated representation widely separates the opercula bordering the insula, the *middle segment of the lateral sulcus* is missing on the inflated reconstruction. Finally, the superior and inferior segments of the

circular sulcus of the insula posteriorly merge to become the ***posterior segment of the lateral sulcus*** [Lat_Fis-post, 41], which curves superiorly to enter the inferior parietal lobule.

The ***central sulcus of the insula*** runs antero-inferiorly from the superior segment of the circular segment of the insula. It is a small sulcus that was not always visible on its whole course on the inflated views. It divides the insula in two parts: ***the short insular gyri*** [G_insular_short, 18] (anterior) and the ***long insular gyrus*** (posterior). Due to their small size, the central sulcus of the insula and the long insular gyri were grouped in the same label [G_Ins_lg_and_S_cent_ins, 17].

2.3 Temporal and occipital lobes

2.3.1 Limits of temporal and occipital lobes—The limits between the *occipital lobe* and the parietal and temporal lobes are partially defined by 2 sulci: the parieto-occipital sulcus or fissure and the temporo-occipital incisure/anterior occipital sulcus. On the midline, the deep ***parieto-occipital sulcus*** [S_parieto_occipital, 65] runs postero-superiorly from the junction of anterior and middle segments of the calcarine sulcus, to the superior edge of the hemisphere. It limits the occipital from the parietal lobe at the medial aspect of the brain. The second relatively clear limit of the occipital lobe is the ***temporo-occipital incisure***, or temporo-occipital notch, a small groove only clearly seen on the *curv* pattern at the inferior edge of the brain. It is described (Duvernoy et al., 1991) as being sometimes continued at the lateral aspect of the brain, by the ***anterior occipital sulcus***. The anterior occipital sulcus and temporo-occipital incisure were grouped in the same label [S_occipital_ant, 59]. They may be connected to several surrounding sulci: superior temporal (R: 8/12; L: 9/12), inferior temporal (R: 5/12; L: 5/12), lateral occipito-temporal (R: 3/12; L: 5/12), inferior occipital (R: 5/12; L: 2/12), or middle occipital (R: 3/12; L: 2/12).

Since there are no other clear limits for the occipital lobe, a virtual line made of 2 segments was drawn on the inflated view to complete these sulcal boundaries (see supplementary material, supp-Fig 2): the first posteriorly concave segment joined the superior tip of the parieto-occipital sulcus, at the superior edge of the hemisphere, to the superior tip of the anterior occipital sulcus/temporo-occipital incisure located infero-lateraly. The second segment was located at the ventro-medial aspect of the brain and ran from the infero-medial tip of the anterior occipital sulcus/temporo-occipital incisure, to the anterior tip of the calcarine sulcus.

Similarly, since no sulcus limits the *temporal from the parietal lobe,* another virtual line was drawn on the inflated view (see supplementary material, supp-Fig 2). This temporo-parietal limit joined the point where the posterior segment of the lateral sulcus curves towards the inferior parietal lobule, to the anterior tip of the middle occipital sulcus. Because the lack of clear limits between the occipital and temporal lobes, they are described together.

2.3.2 Superior aspect of the temporal lobe—The superior aspect of the temporal lobe is a relatively flat area belonging to the ***superior temporal gyrus*** (or T1) that constitutes the temporal operculum and faces the frontal and parietal opercula. Its medial limits are: the inferior segment of the circular sulcus of the insula (antero-medially) and the posterior segment of the lateral sulcus (postero-medially). Its lateral limit was drawn on the "pial" view at the junction between the lateral and superior aspects of the superior temporal gyrus.

The superior aspect of the temporal lobe is divided in 3 parts, anteriorly to posteriorly: the planum polare, the transverse temporal gyrus, and the planum temporale. The ***transverse temporal sulcus*** [S_temporal_transverse, 74] is an important landmark at the superior aspect of the temporal lobe since it divides the planum temporale (posteriorly) from the transverse

temporal gyrus (anteriorly); it originates at the posterior segment of the lateral sulcus, runs anterior and lateral and joins the lateral aspect of the temporal lobe. The ***transverse temporal gyrus*** (or Heschl's gyrus) is a small swelling containing primary auditory cortex, just anterior and parallel to the transverse temporal sulcus. Several "transverse" temporal gyri, bordered by intermediate sulci, are described (Duvernoy et al., 1991), but only the most anterior [G_temp_sup-G_T_transv, 33] corresponds to primary auditory cortex (Shapleske et al., 1999). Conversely, if present, additional transverse temporal gyri, made of secondary auditory cortex (Shapleske et al., 1999), were included in the parcellation planum temporale [G_temp_sup-Plan_tempo, 36]. The ***planum polare*** [G_temp_sup-Plan_polar, 35] is the part of the superior aspect of the superior temporal gyrus located anterior to the transverse temporal gyrus. This flat area reaches the temporal pole anteriorly, and the parahippocampal gyrus medially. Finally the ***planum temporale*** is the part of the superior aspect of the superior temporal gyrus, posterior to the transverse temporal sulcus. Since the posterior segment of the lateral sulcus – which is the medial limit of the planum temporale - curves postero-superiorly, the planum temporale followes this angulation. For this reason the planum temporale is sometimes divided in horizontal and vertical segments but these 2 segments have the same cytoarchitectonics (Shapleske et al., 1999) and were grouped in the same label [G_temp_sup-Plan_tempo, 36].

2.3.3 Lateral aspect of the temporal and occipital lobes—Two aligned sulci, the inferior temporal and inferior occipital sulci, running from the temporal to the occipital poles, limit the lateral from the ventral aspects of the temporal and occipital lobes. The ***inferior temporal sulcus*** [S_temporal_inf, 72] appeared discontinuous and was made of 2 to 7 segments on the inflated view. Since the ***inferior occipital sulcus*** was a small depression difficult to precisely delineate on the inlated view, it was grouped with the corresponding gyrus for labeling [G_and_S_occipital_inf, 2].

The lateral aspect of the temporal lobe is divided in superior and middle temporal gyri by the **superior temporal sulcus** (parallel sulcus) [S_temporal_sup, 73] running parallel to the lateral sulcus, from the temporal pole to the inferior parietal lobule. It branches posteriorly into 2 segments: ascending (angular sulcus) and horizontal. The anterior, horizontal and ascending segments were connected together on the inflated view (R: 5/12; L: 7/12), or remained completely (R: 3/12; L: 2/12) or partially independent. Contrary to other temporal and temporo-occipital sulci, and because of its deepness, the anterior part of the superior temporal sulcus usually appeared continuous (R: 7/12; L: 3/12) or briefly interrupted close to the temporal pole (R: 5/12; L: 6/12). Rarely, it was made of several clearly individualized segments (R: 0/12; L: 3/12). The ***lateral aspect of the superior temporal gyrus*** [G_temp_sup-Lateral, 34], is the only part of the superior temporal gyrus visible on the "pial" view and is connected posteriorly to the inferior parietal lobule. The ***middle temporal gyrus*** (T2) [G_temporal_middle, 38], located between the superior and inferior temporal sulci, is continued posteriorly by the middle occipital gyrus.

Similarly, the lateral aspect of the occipital lobe is divided into superior and middle occipital gyri by the superior occipital sulcus. The ***superior occipital sulcus*** (intraoccipital sulcus) posteriorly continues the intraparietal sulcus and parallels the superior edge of the hemisphere to reach the occipital pole. It is orthogonally crossed by the short ***transverse occipital sulcus*** that extends in the neighboring superior and middle occipital gyri. The superior occipital and transverse occipital sulci were labeled as a whole [S_oc_sup_and_transversal, 58]. The ***superior occipital gyrus*** (O1) [G_occipital_sup, 20] is located superior to the superior occipital sulcus and posteriorly continues the superior parietal gyrus. Its limit from the cuneus was drawn on the "pial" view, as the line following the superior edge of the hemisphere.

The ***middle occipital gyrus*** (O2, lateral occipital gyrus) [G_occipital_middle, 19], located between the superior and inferior occipital sulci covers the major part of the lateral aspect of the occipital lobe. Similarly to the middle frontal gyrus, it contains a ***middle occipital sulcus*** (or lateral occipital sulcus, or prelunatus sulcus) that may anteriorly merge with the horizontal segment of the superior temporal sulcus (R: 2/12; L: 1/12), with the anterior occipital sulcus (R: 1/12; L: 3/12), or with the inferior occipital sulcus (R: 1/12; L: 1/12). Posteriorly it is orthogonally continued by the small and inconstant sulcus lunatus that was difficult to see on the "inflated" view. Middle occipital and lunatus sulci were grouped in the same label [S_oc_middle_and_Lunatus, 57].

2.3.4 Ventral aspect of the temporal and occipital lobes—At the ventral aspects of the hemisphere sulci and gyri follow the axis of the temporo-occipital lobe. Their temporal and occipital parts looks continuous and are only artificially limited from each other (see above, limits of the occipital lobe).

The ventral aspect of the occipito-temporal region is divided by 3 sulci running antero-posteriorly, and comprised from lateral to medial of: (1) the inferior temporal sulcus continuous with the inferior occipital sulcus (previously described as the inferior limit of the lateral aspect of the temporo-occipital region); (2) the lateral occipito-temporal sulcus; and (3) the medial occipito-temporal sulcus. The ***lateral occipito-temporal sulcus*** [S_oc-temp_lat, 60] is discontinuous and difficult to differentiate from the surrounding sulci. It originates close to the inferior occipital gyrus and is limited to the occipital lobe and the posterior part of the temporal lobe without extending to the temporal pole. It could be either independent, or connected to surrounding sulci, including the anterior collateral transverse sulcus (R: 5/12; L: 4/12), the anterior occipital sulcus (R: 3/12; L: 5/12), or the inferior temporal sulcus (R: 1/12; L: 3/12). The ***medial occipito-temporal sulcus*** (collateral sulcus) parallels its lateral counterpart. At its middle third, it gives a branch, the ***lingual sulcus,*** which runs medially into the lingual gyrus. The medial occipito-temporal and lingual sulci were labeled together [S_oc-temp_med_and_Lingual, 61]. Close to the occipital and temporal poles, the medial occipito-temporal sulcus branches into the ***anterior*** [S_collat_transv_ant, 50] ***and posterior transverse collateral sulci*** [S_collat_transv_post, 51].

These sulci delimit 3 occipito-temporal gyri or groups of gyri. The ***inferior occipital gyrus*** (O3) [G_and_S_occipital_inf, 2], and ***inferior temporal gyrus*** (T3) [G_temporal_inf, 37] are the more lateral ones. They are located between the inferior occipital and temporal sulci laterally, and the lateral occipito-temporal and anterior and posterior collateral transverse sulci medially. As previously stated, due to the variability of the inferior occipital sulcus, the inferior occipital sulcus and gyrus were grouped in the same label [G_and_S_occipital_inf, 2]. The ***lateral occipito-temporal gyrus*** (fusiform gyrus, O4-T4) [G_oc-temp_lat-fusiform, 21] is grossly quadrangular and is limited by: the medial occipito-temporal sulcus medially, the anterior transverse collateral sulcus antero-laterally, the lateral occipito-temporal sulcus laterally, and the posterior transverse collateral sulcus postero-laterally. Medial to the medial occipito-temporal sulcus, the medial occipito-temporal gyrus is divided into the lingual (occipital part) and parahippocampal (temporal part) gyri. The ***lingual gyrus*** (O5) [G_oc-temp_med-Lingual, 22] is limited by the calcarine sulcus located above, and by two virtual segments drawn on the pial view. The first one, limiting the lingual gyrus from the occipital pole, joined the medial tip of the posterior transverse collateral sulcus to the posterior tip of the calcarine sulcus. The second segment, delimiting the lingual gyrus from the parahippocampal gyrus, joined the anterior tip of the calcarine sulcus to the medial occipito-temporal sulcus. The ***parahippocampal gyrus*** (or T5) [G_oc-temp_med-Parahip, 23] continues the lingual gyrus anteriorly. The hippocampus, located above the

parahippocampal gyrus, was not labeled because of its complex gray/white organization that did not allow a precise inflation.

2.3.5 Medial aspect of the occipital lobe—The *calcarine sulcus*, a deep fissure located at the medial aspect of the occipital lobe, runs from the region located bellow the splenium of the corpus callosum to the occipital pole. It intersects the parieto-occipital sulcus (see above, limits of the occipital lobe). Anterior to this junction, the calcarine sulcus provides the posterior limit to the postero-ventral part of the cingulate gyrus. Posterior to this junction, it divides the lingual gyrus from the cuneus. The calcarine sulcus is divided in 3 segments in classical descriptions (Duvernoy et al., 1991): anterior (to its junction to the parieto-occipital sulcus), middle, and posterior. The later segment is located close to the occipital pole and corresponds to the inconstant posterior division of the calcarine sulcus into ascending and descending rami. Due to the variability of this posterior segment, the automated labeling procedure was unable to correctly divide the calcarine sulcus in 3 separate segments. We thus included the entire calcarine sulcus within the same label [S_calcarine, 44].

The *cuneus* (O6) [G_cuneus, 11] is uninterruptedly continued by the superior occipital gyrus (O1) at the lateral aspect of the hemisphere. On the pial view, it is a triangle limited by the calcarine sulcus, the parieto-occipital sulcus, and the superior edge of the hemisphere.

2.3.6 Temporal and occipital poles—The temporal and occipital poles are two conic regions, respectively resulting from the fusion of the temporal and occipital gyri. The anterior limit of the *occipital pole* [Pole_occipital, 42] was defined as the circular line joining the posterior tips of the superior, middle, and inferior occipital sulci, the posterior collateral sulcus, and the calcarine sulcus.

Similarly, the *temporal pole* [Pole_temporal, 43] was limited by the circular line joining: the antero-lateral part of the planum polare, the anterior tip of the superior, middle, and inferior temporal sulci, the anterior collateral sulcus and medial occipito-temporal sulcus.

2.4 Parietal lobe

The parietal lobe comprises the lateral and medial aspects of the posterior part of the hemisphere. It is connected to the frontal lobe by two *plis de passage*: the paracentral lobule and the subcentral gyrus.

2.4.1 Lateral aspect of the parietal lobe

2.4.1.1 Lateral limits of the parietal lobe: At the lateral aspect of the brain, the parietal lobe is only clearly limited from the more **anterior** frontal lobe, by the central sulcus. Its *infero-lateral* limit from the temporal lobe was defined as a line joining several anatomical landmarks on the inflated view. From anterior to posterior, this parieto-temporal limit ran from the inferior tip of the central sulcus to the superior tip of the posterior subcentral sulcus; then it followed the posterior segment of the lateral sulcus up to the point where the later curved superiorly, and finally, it reached the anterior tip of the middle occipital sulcus (see supplementary material, supp-Fig 2). As previously described with the temporal and occipital lobes, the *postero-lateral* (parieto-occipital) limit of the parietal lobe was also a virtual line drawn on the inflated view from the superior tip of the anterior occipital sulcus/ temporo-occipital incisure to the superior tip of the parieto-occipital sulcus, located at the superior edge of the hemisphere.

2.4.1.2 Main sulci of the lateral aspect of the parietal lobe: A large and deep sulcal formation made of 2 parts divides the lateral aspect of the parietal lobe: its anterior part, the

postcentral sulcus [S_postcentral, 67] is parallel and posterior to the central sulcus and was made of 2 (R: 7/12; L: 6/12), 1 (R: 4/12; L: 3/12), or 3 segments in our training set (R: 1/12; L: 3/12). Its posterior part, the ***intraparietal sulcus*** (interparietal sulcus) [S_intrapariet_and_P_trans, 56] branches orthogonally from the superior third of the postcentral sulcus, and runs posteriorly, parallel to the superior edge of the hemisphere. The intraparietal sulcus was usually made of several segments on the inflated view: 2 (R: 8/12; L: 9/12), 3 (R: 2/12; L: 2/12), or 1 (R: 2/12; L: 1/12) in our training set. Posterior to the superior tip of the parieto-occipital sulcus, it is continued by the superior occipital sulcus. Additional inconstant sulci, the ***transverse parietal sulci*** are described (Duvernoy et al., 1991). They originate at right angles from the intraparietal sulcus, and may attain the superior edge of the hemisphere, passing through the superior parietal gyrus. Since they were inconstant and branched from the intraparietal sulcus, they were grouped within it in the same label [S_intrapariet_and_P_trans, 56].

The postcentral and intraparietal sulci divide the lateral aspect of the parietal lobe into 3 parts: the postcentral gyrus (anterior), the inferior parietal lobule or P2 (postero-inferior) and the superior parietal lobule or P1 (postero-superior). The inferior parietal lobule is only present at the lateral aspect of the brain whereas the superior parietal lobule also extends to its medial aspect.

2.4.1.3 The post central gyrus: The ***postcentral gyrus*** [G_postcentral, 28] is limited by the central (anteriorly) and postcentral (posteriorly) sulci, and by the 2 lines respectively joining their superior and inferior tips. It is a straight band of cortex, parallel to the precentral, central and post central sulci.

2.4.1.4 The inferior parietal lobule: The ***inferior parietal lobule*** (or P2) is posterior to the postcentral sulcus, and inferior to the intraparietal sulcus. A small sulcus, the ***sulcus intermedius primus*** (of Jensen) [S_interm_prim-Jensen, 55] is perpendicular to the intraparietal sulcus and runs inferiorly, towards the temporal lobe, which it does not reach. It appeared connected to the intraparietal sulcus on the pial view whereas it was usually disconnected from it on the inflated reconstruction (R: 7/12; L: 10/12). The sulcus intermedius primus divides the inferior parietal lobule into supramarginal (anterior) and angular (posterior) gyri.

The ***supramarginal gyrus*** [G_pariet_inf-Supramar, 26] curves around the posterior aspect of the lateral sulcus. The ***angular gyrus*** [G_pariet_inf-Angular, 25] is posterior to the supramarginal gyrus. It was limited by 2 sulci and 2 virtual lines on the inflated view: the intraparietal sulcus and sulcus intermedius primus, and the temporo-parietal and parieto-occipital lines previously described. This quadrangular inflated aspect turns triangular ("angular") on the pial representation, due to cortical folding.

2.4.1.5 The superior parietal lobule: The ***superior parietal lobule*** (or P1) extends to the medial and lateral aspects of the hemisphere. The lateral part of the parietal lobule (superior parietal lobule "per se") [G_parietal_sup, 27] is limited by the intraparietal sulcus inferiorly, the post central sulcus anteriorly, the parieto-occipital limit posteriorly (line between the anterior occipital sulcus and the parieto occipital sulcus), and the superior edge of the hemisphere medially.

2.4.2 Medial aspect of the parietal lobe—The ***precuneus*** [G_precuneus, 30] is the part of the superior parietal lobule (P1) medial to the superior edge of the hemisphere. It is quadrangular and its other boundaries are: posteriorly, the parieto-occipital sulcus (limit from the cuneus); anteriorly, the marginal segment of the cingulate sulcus and the line

joining its superior tip to the superior tip of the post central sulcus (limit from the paracentral gyrus); inferiorly, the subparietal sulcus (limit from the cingulate gyrus).

The *subparietal sulcus* [S_subparietal, 74] posteriorly continues the curve of the cingulate sulcus around the posterior part of the cingulate gyrus. It gives rise to one or several branches directed superiorly that run in the precuneus. On the pial view, this pattern often gives the subparietal sulcus an inverted "T" or "Y" shape.

2.4.3 Fronto-parietal *plis de passage*—Two important *plis de passage*, the paracentral lobule and the subcentral gyrus, connect the frontal and parietal lobes around the central sulcus.The *paracentral lobule* connects the superior parts of the pre and post-central gyri. It is located at the medial aspect of the brain, and is postero-inferiorly limited by the marginal segment of the cingulate sulcus continued by a line running from its posterior tip to the superior tip of the postcentral sulcus. Similarly, its anterior limit is a short vertical or posteriorly concave sulcus, the *paracentral sulcus*, and the 2 lines joining it to the superior tip of the precentral sulcus and to the cingulate sulcus. Finally, its supero-lateral limit was defined as the line joining the superior tip of the precentral, central and post central sulci. Since the paracentral sulcus was often not deep enough to be correctly displayed on the inflated view, the paracentral sulcus and lobule were grouped in the same label [G_and_S_paracentral, 3].

The *subcentral gyrus* (or central operculum), located at the lateral aspect of the brain has a similar organization: it connects the inferior parts of the pre and post central gyri. It is inferiorly limited by the superior part of the circular sulcus of the insula while its superior boundary was defined as a virtual line joining the inferior tip of the precentral, central and post central sulci. The anterior and posterior limits of the subcentral gyrus are two small sulci that may branch from the superior segment of the circular sulcus of the insula or may be independent: the *anterior and posterior subcentral sulci.* Due to this variability of the subcentral sulci, they were grouped with the corresponding gyrus in the same label [G_and_S_subcentral, 4]

2.5 Limbic lobe

The limbic lobe is usually described (Duvernoy et al., 1991) as 2 concentric circles (the limbic and the intralimbic gyri) limited from the surrounding structures by the limbic fissure. The limbic lobe and limbic fissure are two "puzzles" of gyri and sulci arching around the corpus callosum; some of these structures were previously described in this paper.

2.5.1 Limbic fissure—The limbic fissure is described (Duvernoy et al., 1991), as the succession of: the subcallosal, cingulate, subparietal, anterior calcarine, collateral and rhinal sulci. The **subcallosal** (or anterior paraolfactory) and **rhinal** sulci bind the limbic lobe at its 2 extremities but were not deep and long enough to be precisely labeled on the inflated view.

Only the main part of the **cingulate sulcus** (excluding its marginal segment) belongs to the limbic fissure. As previously described, it parallels the anterior and middle parts of the corpus callosum and limits the medial aspect of the frontal lobe from the cingulate gyrus. The cingulate sulcus was discontinuous on the inflated view in about half of the subjects (R: 7/12; L: 5/12). Small accessory sulci originate from the main part of the cingulate sulcus and run superiorly in the medial aspect of the superior frontal gyrus. On the inflated view, these accessory sulci appeared independent from the cingulate sulcus in 8 out of 12 right hemispheres, and in 6 out of 12 left. Rarely (R: 4/12; L: 3/12) the cingulate sulcus was partially doubled by a sulcus running within the cingulate gyrus, the *intracingulate sulcus*. Due to this variability of the cingulate and intracingulate sulci, the anterior and middle parts

of the cingulate gyrus sometime appeared divided into several parts. As a consequence, the cingulate sulcus, intracingulate sulcus and cingulate gyrus were grouped together, and this group of labels was then subdivided in the antero-posterior direction (see bellow limbic gyrus). The cingulate sulcus is continued caudally by the marginal part of the cingulate sulcus [S_cingul-Marginalis, 46] that leaves the limbic fissure to reach the superior edge of the hemisphere, just posterior to the paracentral lobule.

The *subparietal sulcus* [S_subparietal, 71] was described in the parietal lobe section; only its inferior aspect, which more or less follows the curved direction of the middle posterior segment of the cingulate sulcus, belongs to the limbic fissure. The segment of the *calcarine sulcus* anterior to its junction with the parieto-occipital sulcus was the most posterior part of the limbic fissure. It posteriorly limited the ventral division of the posterior segment of the cingulate gyrus. Nevertheless, as previously stated, the calcarine sulcus was labeled as a whole [S_calcarine, 44] Finally, the anterior (temporal) segment of the *medial occipito-temporal sulcus* (or collateral sulcus) [S_oc-temp_med_and_Lingual, 61] inferiorly limits the limbic lobe from the lateral occipito-temporal (or fusiform) gyrus [S_oc-temp_lat, 60].

2.5.2 Limbic gyrus—The limbic gyrus is an arch made of: the subcallosal area, the cingulate gyrus, and the parahippocampal gyrus.

The *subcallosal area* or gyrus [G_subcallosal, 32] is located bellow the genu of the corpus callosum. Its precise limits were difficult to define on the inflated view since it is classically bordered anteriorly by the subcallosal or anterior paraolfactory sulcus which is not deep enough to be seen on the curvature maps. Consequently, arbitrary limits were chosen based on anatomical structures visible on the different representations: inflated view but also pial and native T1 images. It was limited by: the straight line joining the anterior tip of the pericallosal and cingulate sulci, and the posterior tip of the medial orbital sulcus. Posteriorly, the limit was drawn on a parasagittal T1 image as the limit between the cortex and the lamina terminalis.

The *cingulate gyrus* is limited from the corpus callosum by the pericallosal sulcus or sulcus of the corpus callosum [S_pericallosal, 66], from the medial part of the superior frontal gyrus by the cingulate sulcus (anterior, middle anterior and middle-posterior segments), from the precuneus by the subparietal sulcus, and from the lingual part of the medial temporo-occipital gyrus by the anterior part of the calcarine sulcus. As previously stated, the cingulate gyrus, cingulate sulcus and intracingulate sulcus were grouped, and this group of anatomical structures was subdivided in several segments following the antero-posterior direction as proposed by Vogt (Vogt et al., 2003; Vogt et al., 2006): *anterior* (ACC) [G_and_S_cingul-Ant, 6], *middle-anterior* (aMCC) [G_and_S_cingul-Mid-Ant, 7], *middle-posterior* (pMCC) [G_and_S_cingul-Mid-Post, 8], *posterior-dorsal* (dPCC) [G_cingul-Post-dorsal, 9], and *posterior-ventral* (vPCC or isthmus) [G_cingul-Post-ventral, 10]. Vogt defined the Talairach coordinates of the limits between parts of the cingulate gyrus based on cytoarchitectonics and functional arguments: we also used the coronal planes of coordinates y=+30mm, y=+4.5mm, y=−22mm to respectively limit the anterior/middle-anterior, middle-anterior/middle-posterior, and middle-posterior/posterior-dorsal parts of the cingulate gyrus. The posterior-dorsal and posterior-ventral parts of the cingulate gyrus were limited by the horizontal plane of coordinates z=+19.7mm. Finally, the posterior-ventral part of the cingulate gyrus is continued by the *parahippocampal gyrus* (or T5) [G_oc-temp_med-Parahip, 23] that forms the inferior part of the limbic gyrus.

2.5.3 Intralimbic gyrus—The intralimbic gyrus, that classically arches within the limbic gyrus and is made of 3 structures, was not labeled: the **prehippocampal rudiment** and the **indusium griseum** running at the anterior and superior aspects of the corpus callosum were

not visible on the MR scan. Only the **hippocampus** was visible on MR but was not labeled because of its complex grey/white architecture that didn t allow a proper inflation.

2.6 Concordance of Automated/manual labeling

The total average area of the cortex and the proportion of boundaries vertices were similar for right and left hemispheres (table 2). The sulcal cortex represented about 55.5% of the cortical surface.

The global Concordance Index (CI) averaged across subjects after boundary correction (CI_C) (table 2) was 0.84 (standard deviation: 0.024) for the right and 0.85 (standard deviation: 0.017) for the left hemispheres. Not surprisingly, the global CI was reduced when only boundaries were considered. Individual CI_C values are provided for each parcellation unit across the 12 subjects in table 1 and fig. 3. Some small parcellation units had high CI_C values (fig. 4); for instance the areas of the Medial orbital (or olfactory) sulcus [S_orbital_med-olfact, 63] was 5.60 and 5.34 cm^2 for right and left hemispheres and the respective CI_C were 0.96 and 0.95. Conversely, most of the parcellation units with a low CI_C were small structures.

3 Discussion

In classical textbooks (Duvernoy et al., 1991; Ono et al., 1990) and in many atlases used in the neuroimaging community (Desikan et al., 2006; Lancaster et al., 1997; Talairach and Tournoux, 1988), gyri are defined as the cortex joining the bottom of two neighboring sulci, sulci being only consider as virtual landmarks between them. Nevertheless, the brain is more "sulcal" than "gyral", since one half to two thirds of the cortical surface is hidden in the sulci and in the lateral fossa of the brain (Van Essen, 2005; Zilles et al., 1997). This deep anatomy only recently became clear thanks to medical imaging and computer engineering that allowed the development of inflated and flattened maps of the cortical surface of the human brain (Dale et al., 1999; Dale and Sereno, 1993; Fischl et al., 1999a; Fischl et al., 1999b; Van Essen, 2005). Surface based cortical labeling methods have major advantages as compared to volume based methods; first, the complex folded anatomy of the human cerebral cortex, which makes the identification of sulco-gyral structures difficult, even by trained anatomists, is visually simplified by the inflation process. For instance, the anatomy of the occipital pole is usually not clearly described in classical textbooks (Carpenter, 1991; Federative Committee on Anatomical Terminology, 1998; Ono et al., 1990), whereas cortical inflation clearly reveals a robust organization in 3 parallel gyri, similar to the one previously described by Duvernoy (Duvernoy et al., 1991). The description of the lateral sulcus is also aided by the use of inflated maps as the entire -usually hidden- cortex of the insula and the opercula is exposed and parcellated on a single view. Second, interindividual differences in cortical anatomy are better taken in account in surface versus volume approaches. For instance, Talairach (Talairach and Szikla, 1967) studied the location of the central sulcus in 20 hemispheres after they were registered in the AC-PC coordinate system: a variation of several centimeters in the antero-posterior location of the central sulcus was observed, though this sulcus is regarded as one of the most constant. Not surprisingly, since they use maps of cortical geometry to drive cross-subject registration, group average using surface based approaches give a markedly better alignment of sulco-gyral structures than volume-based methods (Fischl et al., 1999b; Van Essen, 2005). Third, compared to a classical orthogonal volume coordinate system, a surface coordinate system respects cortical topology: points with close surface coordinates are always close on the cortical surface, whereas points with similar Talairach coordinates may be widely separated on the cortical surface (Fischl et al., 1999b; Van Essen et al., 1998).

Despite these substantial advantages for analyzing, averaging and displaying data, cortical inflation software creates new representations of cortical anatomy that the users need to relearn. For this purpose, tools for automatically labeling the cortical surface should provide great help; for instance, the FreeSurfer package http://surfer.nmr.mgh.harvard.edu/ is a set of tools for fully automated volume and surface reconstruction and labeling. This paper presents the anatomical rules and nomenclature used to build the sulco-gyral atlas included in this package. It contains minor changes as compared to versions included in prior distributions. To date, the FreeSurfer package, including the current or a previous version of the atlas was individually licensed 6700 times.

Classical anatomical textbooks (Duvernoy et al., 1991; Talairach and Szikla, 1967; Talairach and Tournoux, 1988) and most of the available atlases (Desikan et al., 2006; Lancaster et al., 2000; Shattuck et al., 2008) use a gyral based parcellation of the brain. Since a large proportion of the brain is hidden in sulci and lateral fossa (Van Essen, 2005; Zilles et al., 1997), other authors proposed a sulcal-based parcellation (Rettmann et al., 2005; Tosun et al., 2004). In this paper we proposed a mixed, sulco-gyral-based parcellation: the gyral cortex was defined as the one seen on a 3D reconstruction before inflation (pial view), the remaining hidden part being conversely labeled sulcal. A similar sulco-gyral classification was proposed as a starting point for a sulcal segmentation using a deformable surface model (Rettmann et al., 2002). In this approach, a deformable surface, similar to a flexible balloon, surrounded one hemisphere. This balloon was progressively deflated and the deflation was stopped as its surface matched the cortical surface. Due to this process the content of the lateral fossa of the brain was classified as sulcal although it also contained both gyral and sulcal elements.

In order to obtain a better sulco-gyral classification, including for the cerebral lateral fossa, we used two parameters computed from the cortical surface: the mean curvature and the average convexity. The latter gave a good sulco-gyral classification except for the lateral fossa whose deep location would have resulted in the labeling of all structures forming and bordering the insula as sulcal, including the insular gyri and deeper part of the opercula. Thus, the structures of the lateral fossa were classified based upon their mean curvature value, some being considered as sulcal (circular sulcus of the insula…), and others being labeled gyral (insular gyri, superior aspect of the superior temporal gyrus…). This process resulted in about 55.5% of hidden cortex for both hemispheres, which is slightly lower than previously published results estimating that about 60% of the cortex is buried (Van Essen, 2005; Zilles et al., 1997). This value is highly dependent upon the precise value of the average convexity used as a threshold to perform the sulco-gyral classification. Although anatomically relevant, since it gave a reasonable sulco-gyral classification on the pial views (fig. 2), the threshold we used probably explains this "over representation" of gyral cortex in our parcellation.

Out method subparcellates the sulcal and gyral parts of the cortex into smaller entities based on classical anatomical descriptions. We mainly used Duvernoy s nomenclature (Duvernoy et al., 1991) since it gives a simple but precise description of the entire cortical surface based on 18 brains, and because it is widely and internationally used. This nomenclature includes and completes terms provided by the TA (Federative Committee on Anatomical Terminology, 1998). When necessary, the correspondence with other terminologies (Ono et al., 1990) was indicated to help the reader who is familiar with them. The final result was a parcellation of the entire cortex 74 different structures. This high number of anatomical regions allows a more precise description of the cortical surface, with acceptable automated/ manual concordance. By comparison, the Talairach Daemon (Lancaster et al., 1997) and the surface-based parcellation proposed by Desikan (Desikan et al., 2006) defined 48 and 34 gyral regions per hemisphere respectively.

While the subparcellation we performed was only driven by anatomical conventions, other methods have been proposed. For instance in a watershed based approach (Rettmann et al., 2002; Rettmann et al., 2005) the sulcal cortex is subparcellated in catchment basins defined by the geodesic distance from the bottom of the sulcus to the cortical surface. This approach allows a semi-automated segmentation of branching sulci, for instance superior frontal and precentral sulci. Nevertheless, this approach sometimes misses limits between sulci and a manual intervention is needed (Rettmann et al., 2005).

In another approach (Cachia et al., 2003), bottom lines at the sulcal fundi are first delineated using a contextual pattern recognition method. A pair of these bottom lines were then used as a starting point for a Voronoï diagram to localize the crown of the gyrus limited by these two lines. Finally, once the crowns of the gyri are located, another set of Voronoï diagrams is built to delineate the corresponding gyri. While this method is presented as automated, the definition of the pairs of sulci initially used as starting points remains manual.

Since we aimed to provide a familiar and standard parcellation scheme to the users, the limits between cortical structures we proposed were only based on anatomical conventions similar to the ones used in classical textbooks (Duvernoy et al., 1991). The labeling of the 12 subjects used to build the atlas was completely manual, with the attendant possible variations of the boundaries between same structures across subjects. Nevertheless, the parcellation was performed by the same author, and cortical structures were labeled in the same order for each subject. Moreover, this manual labeling was not directly used to label "new" hemispheres, but was only one of the parameters used to train the parcellation program that also integrated other parameters, especially the geometry of the cortical surface, and the relative location of the cortical structures (Fischl et al., 2002; Fischl et al., 2004).

One major limitation to this surface atlas is that it only labels the cortex, ignoring subcortical structures and hippocampus. Nevertheless, in the FreeSurfer reconstruction stream, deep structures are labeled by a volume-based tool using a similar probabilistic algorithm (Fischl et al., 2002), resulting in the labeling of cortical as well as subcortical and ventricular structures at the end of the process.

The automatic labeling algorithm used for this paper was previously published using the same set of brains (Fischl et al., 2004) with similar results for the average CI_O: 80% for the left hemisphere and 79% for the right hemisphere. Because this paper is derived from the same dataset, and a very slightly modified parcellation scheme, we did not seek to extensively validate the technique again. Since the precision of the manual definition of boundaries on the cortical surface is obviously limited by the width of the lines drawn to limit contiguous labels, the CI were also computed without considering their boundaries (CI_C). This better evaluates the auto/manual concordance since a discordance located just at the border between two areas has negligible anatomical or functional significance. After correction for this "border effect", CI_C (percentage of area identically labeled by the manual and automated procedure) was close to 85% for both hemispheres, with noteworthy differences between structures (fig. 3 and table 1). Lower CI_C values were found for variable/inconstant structures (anterior occipital sulcus, sulcus intermedius primus, suborbital sulcus...), for structures without clear landmarks (subcallosal area), and for sulci not deep enough to be correctly and constantly recognized (subcentral and paracentral sulci, central sulcus of the insula…). The structure area s was another important factor determining its concordance (fig. 4); the area of 27 out of 33 cortical structures with a CI_C lower than 0.75, was lower than 11 cm^2. Some structures with reproducibly low CI_C values across subjects were grouped to increase robustness of the labeling procedure. Conversely, other structures that are known to be less variable across individuals had noticeable high CI_C

(e.g. central, pre and post central gyri, calcarine sulcus, orbital H-shaped sulcus, superior temporal sulcus).

To our knowledge, this paper is the first extensive description of the anatomical conventions used to build a probabilistic sulco-gyral atlas of the human cerebral cortex. Even for well trained neuroanatomists, manual labeling of the cortex reconstructed from one given MR scan remains challenging: it is time consuming, it implies a high degree of anatomical expertise and remains sensitive to labeling variations. Using a fully automated approach to label the same scan is more reproducible and practical for large datasets. Manual localization of sulco-gyral structure remains difficult even on inflated maps and is often a compromise between several possible labelings; the automated procedure usually selects one alternative labeling scheme that on visual examination by an expert anatomist is found to be acceptable. For this reason, and despite a lack of perfect concordance between automated versus manual labeling, the proposed atlas produces an acceptable, reproducible and rapid labeling of the entire cortical surface. It produces a detailed parcellation of the cortex into 74 different structures per hemisphere that may be used for morphological and functional analysis. This paper will also serve as a reference for users of this automated tool since it provides a precise description of each of the parcellations that are output from the FreeSurfer surface reconstruction stream.

Supplementary Material

Refer to Web version on PubMed Central for supplementary material.

Acknowledgments

References

Broca P. Sur la nomenclature cérébrale. Bull Soc Anthropol Paris. 1877; 12:614–618.

Broca P. Nomenclature Cérébrale. Dénomination des divisions et subdivisions des hémisphères et des anfractuosités de leur surface. Revue d'anthropologie 2ème série. 1878:193–236.

Cachia A, Mangin JF, Riviere D, Papadopoulos-Orfanos D, Kherif F, Bloch I, Regis J. A generic framework for the parcellation of the cortical surface into gyri using geodesic Voronoi diagrams. Med Image Anal. 2003; 7:403–416. [PubMed: 14561546]

Carpenter, M. core text of neuroanatomy. 4. Williams & Wilkins; Baltimore: 1991.

Caviness VS, Meyer J, Makris N, Kennedy DN. MRI-Based Topographic Parcellation of Human Neocortex: An Anatomically specified Method with Estimate of Reliability. J Cogn Neurosci. 1996; 8:566–587.

Dale AM, Fischl B, Sereno MI. Cortical surface-based analysis. I. Segmentation and surface reconstruction. Neuroimage. 1999; 9:179–194. [PubMed: 9931268]

Dale AM, Sereno MI. Improved Localization of Cortical Activity by Combining EEG and MEG with MRI Cortical Surface Reconstruction: A Linear Approach. Neuroscience. 1993; 5:2, 162–176.

Desikan RS, Segonne F, Fischl B, Quinn BT, Dickerson BC, Blacker D, Buckner RL, Dale AM, Maguire RP, Hyman BT, Albert MS, Killiany RJ. An automated labeling system for subdividing the human cerebral cortex on MRI scans into gyral based regions of interest. Neuroimage. 2006; 31:968–980. [PubMed: 16530430]

Destrieux, C.; Halgren, E.; Fischl, B.; Sereno, MI. Soc Neurosci. Los Angeles, CA: 1998. Variability of the human brain studied on the flattened cortical surface; p. 1164

Duvernoy, HM.; Cabanis, EA.; Vannson, JL. The Human brain: surface, three-dimensional sectional anatomy and MRI. Springer-Verlag; Wien: 1991.

Ecker, A. The Cerebral convolutions of man: represented according to original observations, especially upon their development in the foetus, intended for the use of physicians. Appleton & Co; New York: 1873.

Federative Committee on Anatomical Terminology. Terminologia anatomica: international anatomical terminology. Thieme; Stuttgart; New York: 1998.

Fischl B, Salat DH, Busa E, Albert M, Dieterich M, Haselgrove C, van der Kouwe A, Killiany R, Kennedy D, Klaveness S, Montillo A, Makris N, Rosen B, Dale AM. Whole brain segmentation: automated labeling of neuroanatomical structures in the human brain. Neuron. 2002; 33:341–355. [PubMed: 11832223]

Fischl B, Sereno MI, Dale AM. Cortical surface-based analysis. II: Inflation, flattening, and a surface-based coordinate system. Neuroimage. 1999a; 9:195–207. [PubMed: 9931269]

Fischl B, Sereno MI, Tootell RB, Dale AM. High-resolution intersubject averaging and a coordinate system for the cortical surface. Hum Brain Mapp. 1999b; 8:272–284. [PubMed: 10619420]

Fischl B, van der Kouwe A, Destrieux C, Halgren E, Segonne F, Salat DH, Busa E, Seidman LJ, Goldstein J, Kennedy D, Caviness V, Makris N, Rosen B, Dale AM. Automatically parcellating the human cerebral cortex. Cereb Cortex. 2004; 14:11–22. [PubMed: 14654453]

Gall, F. Craniologie ou découvertes nouvelles du Docteur F.J. Gall, concernant le cerveau, le crâne, et les organes. Nicolle; Paris: 1807.

Gratiolet, P. Mémoire sur les plis cérébraux de l'homme et des primates. Arthus Bertrand; Paris: 1854.

Kachlik D, Baca V, Bozdechova I, Cech P, Musil V. Anatomical terminology and nomenclature: past, present and highlights. Surg Radiol Anat. 2008; 30:459–466. [PubMed: 18488135]

Lancaster J, Rainey LH, Summerlin JL, Freitas CS, Fox P, Evans A, Toga AW, Mazziotta JC. Automated Labeling of the human Brain: A Preliminary Report on the Development and Evaluation of a Forward-Transform Method. Hum Brain Mapp. 1997; 5:238–242. [PubMed: 20408222]

Lancaster JL, Woldorff MG, Parsons LM, Liotti M, Freitas CS, Rainey L, Kochunov PV, Nickerson D, Mikiten SA, Fox PT. Automated Talairach atlas labels for functional brain mapping. Hum Brain Mapp. 2000; 10:120–131. [PubMed: 10912591]

Leuret, F.; Gratiolet, P. Anatomie comparée du système nerveux, considéré dans ses rapports avec l'intelligence. Baillière; Paris: 1839.

Ono, M.; Kubik, S.; Abernathey, CD. Atlas of the cerebral sulci. G. Thieme Verlag; New York: Thieme Medical Publishers; Stuttgart: 1990.

Rettmann ME, Han X, Xu C, Prince JL. Automated sulcal segmentation using watersheds on the cortical surface. Neuroimage. 2002; 15:329–344. [PubMed: 11798269]

Rettmann ME, Tosun D, Tao X, Resnick SM, Prince JL. Program for Assisted Labeling of Sulcal Regions (PALS): description and reliability. Neuroimage. 2005; 24:398–416. [PubMed: 15627582]

Segonne F, Dale AM, Busa E, Glessner M, Salat D, Hahn HK, Fischl B. A hybrid approach to the skull stripping problem in MRI. Neuroimage. 2004; 22:1060–1075. [PubMed: 15219578]

Segonne F, Pacheco J, Fischl B. Geometrically accurate topology-correction of cortical surfaces using nonseparating loops. IEEE Trans Med Imaging. 2007; 26:518–529. [PubMed: 17427739]

Shapleske J, Rossell SL, Woodruff PW, David AS. The planum temporale: a systematic, quantitative review of its structural, functional and clinical significance. Brain Res Brain Res Rev. 1999; 29:26–49. [PubMed: 9974150]

Shattuck DW, Mirza M, Adisetiyo V, Hojatkashani C, Salamon G, Narr KL, Poldrack RA, Bilder RM, Toga AW. Construction of a 3D probabilistic atlas of human cortical structures. Neuroimage. 2008; 39:1064–1080. [PubMed: 18037310]

Talairach, J.; Szikla, G. Atlas d'anatomie stéréotaxique du télencéphale; études anatomo-radiologiques. Masson; Paris: 1967.

Talairach, J.; Tournoux, P. Co-planar stereotaxic atlas of the human brain: 3-dimensional proportional system: an approach to cerebral imaging. G. Thieme; New York: Thieme Medical Publishers; Stuttgart; New York: 1988.

Thompson PM, Woods RP, Mega MS, Toga AW. Mathematical/computational challenges in creating deformable and probabilistic atlases of the human brain. Hum Brain Mapp. 2000; 9:81–92. [PubMed: 10680765]

Tosun D, Rettmann ME, Han X, Tao X, Xu C, Resnick SM, Pham DL, Prince JL. Cortical surface segmentation and mapping. Neuroimage. 2004; 23(Suppl 1):S108–118. [PubMed: 15501080]

Van Essen DC. A Population-Average, Landmark- and Surface-based (PALS) atlas of human cerebral cortex. Neuroimage. 2005; 28:635–662. [PubMed: 16172003]

Van Essen DC, Drury HA. Structural and functional analyses of human cerebral cortex using a surface-based atlas. J Neurosci. 1997; 17:7079–7102. [PubMed: 9278543]

Van Essen DC, Drury HA, Joshi S, Miller MI. Functional and structural mapping of human cerebral cortex: solutions are in the surfaces. Proc Natl Acad Sci U S A. 1998; 95:788–795. [PubMed: 9448242]

Vesale, A. Résumé de ses livres sur la fabrique du corps humain. Les Belles lettres; Paris: 2008.

Vesalius, A. [Ex officina I. Oporini; Basileae: 1543. De humani corporis fabrica libri septem; p. 659(i.e. 663) p

Vogt BA, Berger GR, Derbyshire SW. Structural and functional dichotomy of human midcingulate cortex. Eur J Neurosci. 2003; 18:3134–3144. [PubMed: 14656310]

Vogt BA, Vogt L, Laureys S. Cytology and functionally correlated circuits of human posterior cingulate areas. Neuroimage. 2006; 29:452–466. [PubMed: 16140550]

Whitmore I. Terminologia anatomica: new terminology for the new anatomist. Anat Rec. 1999; 257:50–53. [PubMed: 10321431]

Zilles K, Schleicher A, Langemann C, Amunts K, Morosan P. Quantitative analysis of sulci in the human cerebral cortex: development, regional heterogeneity, gender difference, asymetry, intersubject variability and cortical architecture. Hum Brain Mapp. 1997; 5:218–221. [PubMed: 20408218]
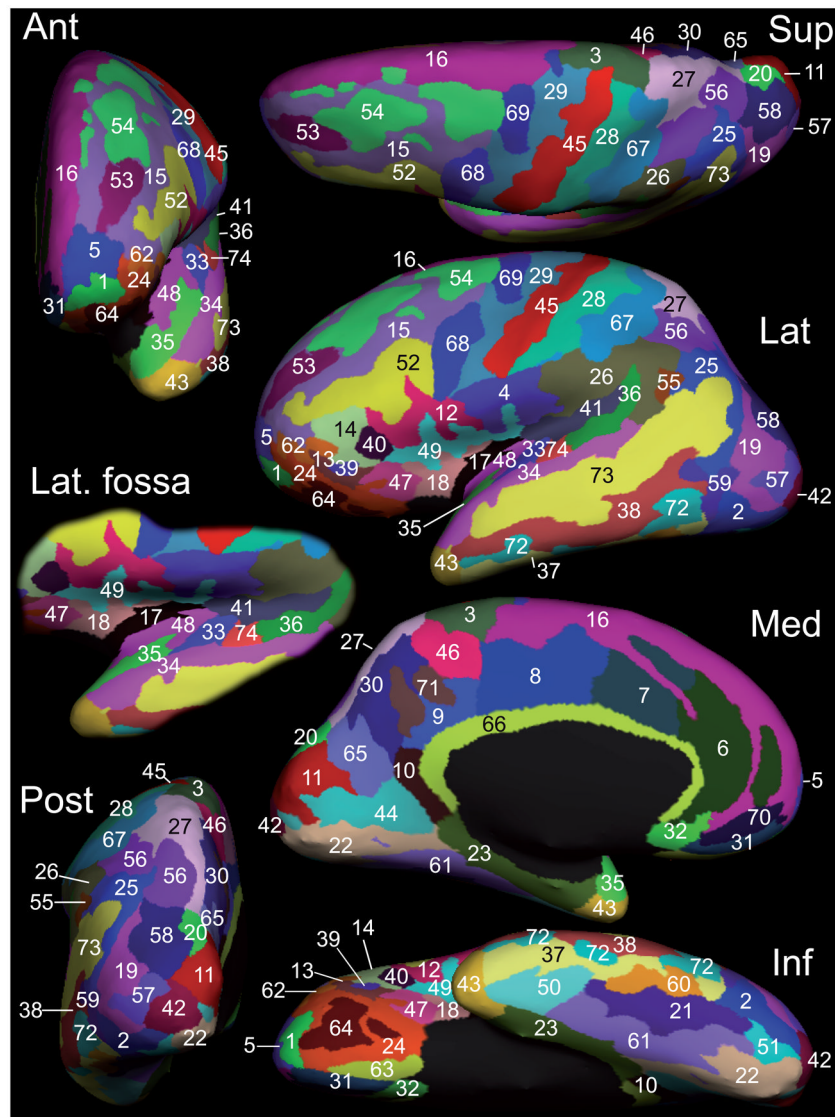
Figure 1. Inflated view of the manual parcellation of one hemisphere of the Training set
Numerical indices refer to the anatomical regions defined in Table 1: superior (Sup),
anterior (Ant), lateral (Lat), posterior (Post), medial (Med), and inferior views are provided.
Both gyral and sulcal cortices are visible on this representation. The lateral fossa is
displayed on a separate lateral view (Lat. fossa) oriented to better show: the insula (17:
central S. and long insular G., 18: short insular G) limited by the circular sulcus of the insula
(47: ant, 48: inf, 49: sup), and the superior aspect of the superior temporal gyrus (35: planum
polare, 33: transverse temporal G., 74: transverse temporal S, 36: planum polare). The
inflated lateral views of all 12 subjects are shown in supplementary figures 3A and 3B; the
inflated medial views in supplementary figures 4A and 4B.
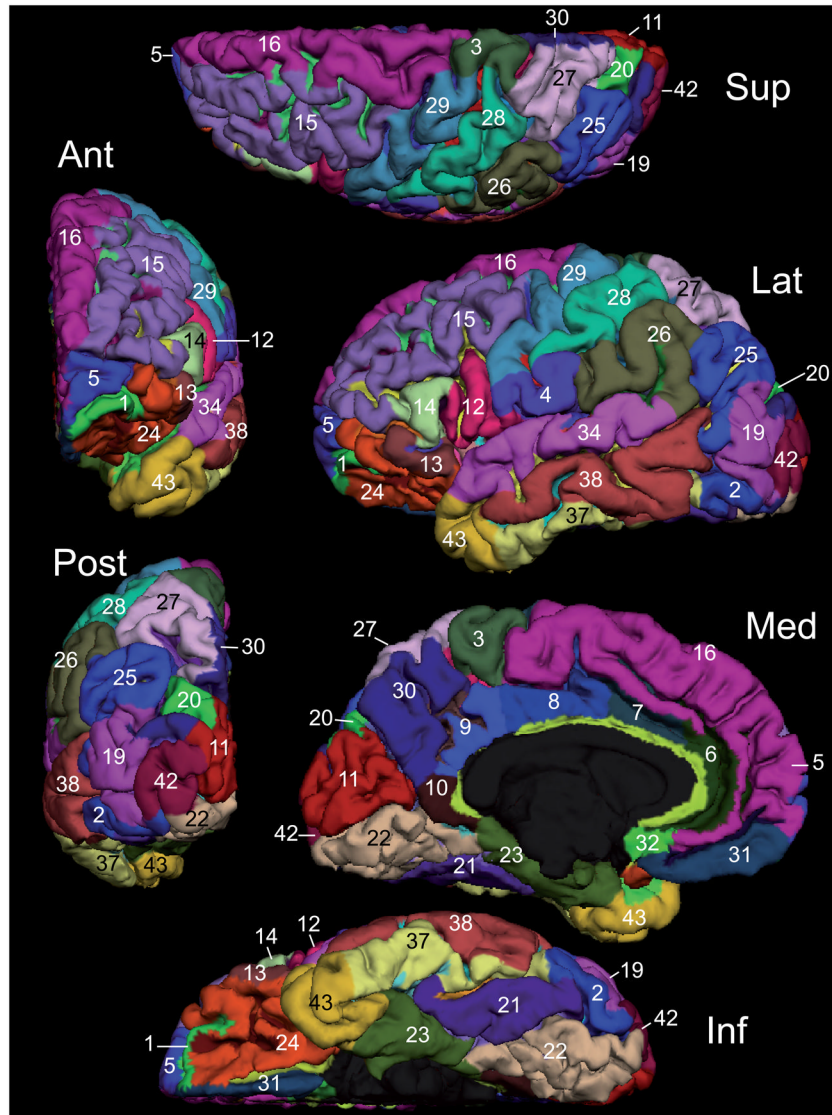
Figure 2. pial view of the manual parcellation of one hemisphere of the Training set
Numerical indices refer to the anatomical regions defined in Table 1: superior (Sup), anterior (Ant), lateral (Lat), posterior (Post), medial (Med), and inferior views are provided. Notice that the sulcal cortex is mostly invisible on this representation of the cortical surface. The pial lateral views of all 12 subjects are shown in supplementary figures 5A and 5B; the pial medial views in supplementary figures 6A and 6B.
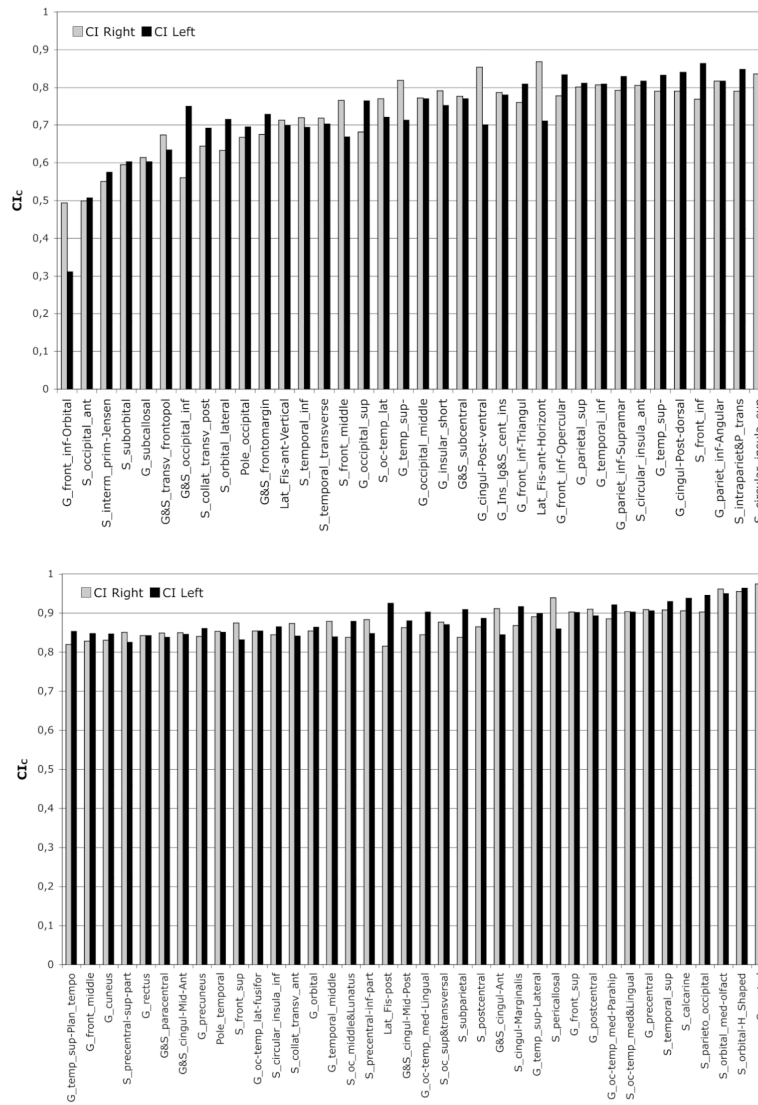
Figure 3. CI values for each of the 74 labels across the 12 subjects

A CI after boundary correction (CI_C) was computed for right and left hemisphere across the 12 subjects for each of the 74 anatomical labels. Results are presented in increasing values of CI.
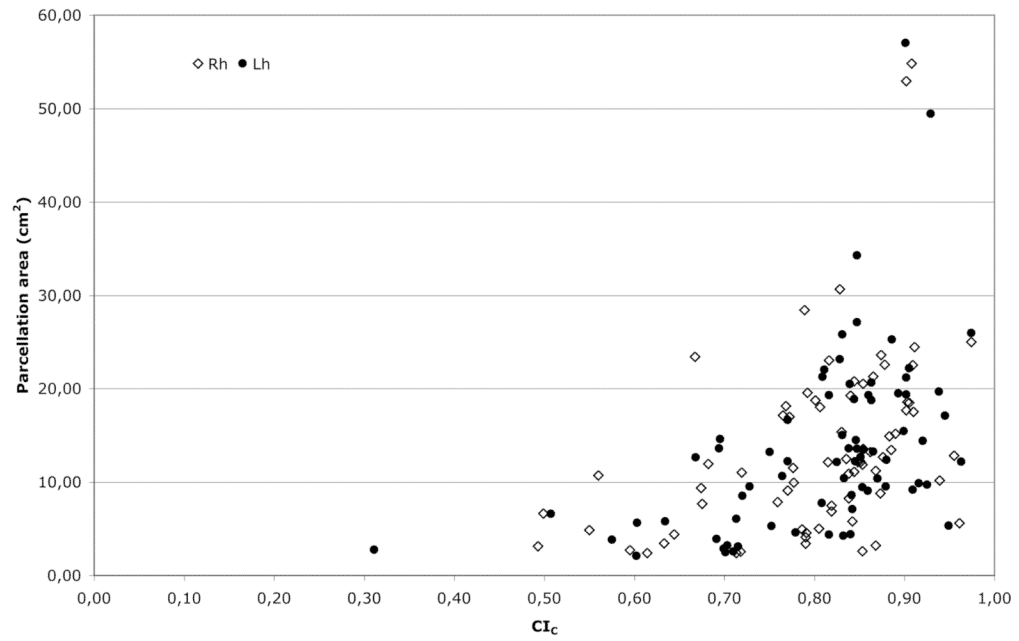
Figure 4. Plot of the area and CIc
The average area was plotted against the average concordance index after boundary correction (CIc) for each of the 74 parcellation units in the right (rh) and left (lh) hemispheres.

Table 1

List of anatomical parcellations.

index	Short Name	Long name (TA nomenclature is bold typed)	Visible on views	CI_C		area (cm²)	
				Rh	Lh	Rh	Lh
1	G_and_S_frontomargin	Fronto-marginal gyrus (of Wernicke) and sulcus	A, L, I	0.68	0.73	7.71	9.55
2	G_and_S_occipital_inf	Inferior occipital gyrus (O3) and sulcus	L, P, I	0.56	0.75	10.74	13.22
3	G_and_S_paracentral	*Paracentral lobule and sulcus*	S, P, M	0.85	0.84	12.18	13.62
4	G_and_S_subcentral	Subcentral gyrus (central operculum) and sulci	L	0.78	0.77	11.54	12.24
5	G_and_S_transv_frontopol	Transverse frontopolar gyri and sulci	A, L, M, I	0.67	0.63	9.39	5.80
6	G_and_S_cingul-Ant	Anterior part of the *cingulate gyrus and sulcus* (ACC)	M	0.91	0.84	24.49	18.89
7	G_and_S_cingul-Mid-Ant	Middle-anterior part of the *cingulate gyrus and sulcus* (aMCC)	M	0.85	0.85	12.32	12.23
8	G_and_S_cingul-Mid-Post	Middle-posterior part of the *cingulate gyrus and sulcus* (pMCC)	M	0.86	0.88	13.25	12.38
9	G_cingul-Post-dorsal	Posterior-dorsal part of the *cingulate gyrus* (dPCC)	M	0.79	0.84	4.12	4.44
10	G_cingul-Post-ventral	Posterior-ventral part of the cingulate gyrus (vPCC, *isthmus of the cingulate gyrus*)	M, I	0.85	0.70	2.61	2.50
11	G_cuneus	*Cuneus* (O6)	S, P, M	0.83	0.85	15.41	14.52
12	G_front_inf-Opercular	*Opercular part of the inferior frontal gyrus*	L, I	0.78	0.83	9.98	10.43
13	G_front_inf-Orbital	*Orbital part of the inferior frontal gyrus*	L, I	0.49	0.31	3.15	2.77
14	G_front_inf-Triangul	*Triangular part of the inferior frontal gyrus*	L, I	0.76	0.81	7.88	7.79
15	G_front_middle	*Middle frontal gyrus* (F2)	S, A, L	0.83	0.85	30.67	34.29
16	G_front_sup	*Superior frontal gyrus* (F1)	S, A, L, M	0.90	0.90	52.97	57.05
17	G_Ins_lg_and_S_cent_ins	*Long insular gyrus and central sulcus of the insula*	L	0.79	0.78	4.98	4.61
18	G_insular_short	*Short insular gyri*	L	0.79	0.75	4.58	5.32
19	G_occipital_middle	Middle occipital gyrus (O2, lateral occipital gyrus)	S, L, P	0.77	0.77	17.01	16.68
20	G_occipital_sup	Superior occipital gyrus (O1)	S, L, P	0.68	0.76	11.98	10.66
21	G_oc-temp_lat-fusifor	*Lateral occipito-temporal gyrus* (fusiform gyrus, O4-T4)	I	0.85	0.85	13.60	13.48
22	G_oc-temp_med-Lingual	*Lingual gyrus*, ligual part of the *medial occipito-temporal gyrus*, (O5)	P, M, I	0.84	0.90	20.82	21.22
23	G_oc-temp_med-Parahip	*Parahippocampal gyrus*, parahippocampal part of the *medial occipito-temporal gyrus*, (T5)	M, I	0.89	0.92	13.48	14.44
24	G_orbital	*Orbital gyri*	A, L, I	0.85	0.86	20.57	18.79
25	G_pariet_inf-Angular	*Angular gyrus*	S, L, P	0.82	0.82	23.07	19.32
26	G_pariet_inf-Supramar	*Supramarginal gyrus*	S, L, P	0.79	0.83	19.58	23.18
27	G_parietal_sup	*Superior parietal lobule* (lateral part of P1)	S, L, P, M	0.80	0.81	18.77	22.04

index	Short Name	Long name (TA nomenclature is bold typed)	Visible on views	CI_C		area (cm²)	
				Rh	Lh	Rh	Lh
28	G_postcentral	**Postcentral gyrus**	S, L, P	0.91	0.89	17.55	19.53
29	G_precentral	**Precentral gyrus**	S, A, L	0.91	0.91	22.55	22.22
30	G_precuneus	**Precuneus** (medial part of P1)	S, P, M	0.84	0.86	19.26	19.32
31	G_rectus	**Straight gyrus**, Gyrus rectus	A, M, I	0.84	0.84	5.80	7.11
32	G_subcallosal	**Subcallosal area, subcallosal gyrus**	M, I	0.61	0.60	2.41	2.13
33	G_temp_sup-G_T_transv	**Anterior transverse temporal gyrus** (of Heschl)	A, L	0.79	0.83	3.42	4.27
34	G_temp_sup-Lateral	Lateral aspect of the **superior temporal gyrus**	A, L	0.89	0.90	15.20	15.46
35	G_temp_sup-Plan_polar	Planum polare of the **superior temporal gyrus**	A, L, M	0.82	0.71	6.90	6.08
36	G_temp_sup-Plan_tempo	**Planum temporale or temporal plane** of the superior temporal gyrus	A, L	0.82	0.85	7.52	9.48
37	G_temporal_inf	**Inferior temporal gyrus** (T3)	L, I	0.81	0.81	18.05	21.27
38	G_temporal_middle	**Middle temporal gyrus** (T2)	A, L, P, I	0.88	0.84	22.59	20.52
39	Lat_Fis-ant-Horizont	Horizontal ramus of the **anterior segment of the lateral sulcus** (or fissure)	L, I	0.87	0.71	3.22	2.59
40	Lat_Fis-ant-Vertical	Vertical ramus of the **anterior segment of the lateral sulcus** (or fissure)	L, I	0.71	0.70	2.43	2.87
41	Lat_Fis-post	**Posterior ramus** (or segment) **of the lateral sulcus** (or fissure)	A, L	0.82	0.93	12.15	9.73
42	Pole_occipital	**Occipital pole**	L, P, M, I	0.67	0.70	23.43	14.62
43	Pole_temporal	**Temporal pole**	A, L, M, I	0.85	0.85	11.91	12.71
44	S_calcarine	**Calcarine sulcus**	M	0.91	0.94	18.51	19.69
45	S_central	**Central sulcus** (Rolando's fissure)	S, A, L, P	0.97	0.97	25.02	25.98
46	S_cingul-Marginalis	**Marginal branch** (or part) **of the cingulate sulcus**	S, P, M	0.87	0.92	11.23	9.88
47	S_circular_insula_ant	Anterior segment of the **circular sulcus of the insula**	L, I	0.81	0.82	5.05	4.39
48	S_circular_insula_inf	Inferior segment of the **circular sulcus of the insula**	A, L	0.84	0.87	11.13	13.27
49	S_circular_insula_sup	Superior segment of the **circular sulcus of the insula**	L, I	0.84	0.83	12.50	15.06
50	S_collat_transv_ant	Anterior transverse collateral sulcus	I	0.87	0.84	8.81	8.63
51	S_collat_transv_post	Posterior transverse collateral sulcus	I	0.64	0.69	4.43	3.93
52	S_front_inf	**Inferior frontal sulcus**	S, A, L	0.77	0.86	18.17	20.68
53	S_front_middle	Middle frontal sulcus	S, A, L	0.77	0.67	17.16	12.65
54	S_front_sup	**Superior frontal sulcus**	S, A, L	0.87	0.83	23.64	25.82
55	S_interm_prim-Jensen	Sulcus intermedius primus (of Jensen)	S, L, P	0.55	0.58	4.88	3.83
56	S_intrapariet_and_P_trans	**Intraparietal sulcus** (interparietal sulcus) and transverse parietal sulci	S, L, P	0.79	0.85	28.44	27.14
57	S_oc_middle_and_Lunatus	Middle occipital sulcus and lunatus sulcus	S, L, P	0.84	0.88	8.29	9.55

index	Short Name	Long name (TA nomenclature is bold typed)	Visible on views	CI_C		area (cm²)	
				Rh	Lh	Rh	Lh
58	S_oc_sup_and_transversal	Superior occipital sulcus and *transverse occipital sulcus*	S, L, P	0.88	0.87	12.70	10.38
59	S_occipital_ant	Anterior occipital sulcus and *preoccipital notch* (temporo-occipital incisure)	L, P	0.50	0.51	6.64	6.60
60	S_oc-temp_lat	Lateral occipito-temporal sulcus	I	0.77	0.72	9.13	8.53
61	S_oc-temp_med_and_Lingual	Medial occipito-temporal sulcus (*collateral sulcus*) and lingual sulcus	M, I	0.90	0.90	18.57	19.40
62	S_orbital_lateral	Lateral orbital sulcus	A, L, I	0.63	0.72	3.46	3.13
63	S_orbital_med-olfact	Medial orbital sulcus (*olfactory sulcus*)	I	0.96	0.95	5.60	5.34
64	S_orbital-H_Shaped	*Orbital sulci* (H-shaped sulci)	I, L	0.96	0.96	12.84	12.19
65	S_parieto_occipital	*Parieto-occipital sulcus* (or fissure)	S, P, M	0.90	0.95	17.70	17.13
66	S_pericallosal	Pericallosal sulcus (*S of corpus callosum*)	M	0.94	0.86	10.21	9.08
67	S_postcentral	*Postcentral sulcus*	S, L, P	0.87	0.89	21.32	25.27
68	S_precentral-inf-part	Inferior part of the *precentral sulcus*	S, A, L	0.88	0.85	14.92	13.58
69	S_precentral-sup-part	Superior part of the *precentral sulcus*	S, L	0.85	0.83	12.16	12.16
70	S_suborbital	Suborbital sulcus (sulcus rostrales, supraorbital sulcus)	M	0.60	0.60	2.74	5.67
71	S_subparietal	*Subparietal sulcus*	M	0.84	0.91	10.92	9.21
72	S_temporal_inf	*Inferior temporal sulcus*	L, P, I	0.72	0.69	11.04	13.63
73	S_temporal_sup	*Superior temporal sulcus* (parallel sulcus)	S, A, L, P	0.91	0.93	54.83	49.45
74	S_temporal_transverse	*Transverse temporal sulcus*	A, L	0.72	0.70	2.59	3.24

This table refers to the final parcellation scheme used on our Training set (see method) to build the automated labeling software included in the FreeSurfer package since August 2009 (Freesurfer v4.5, aparc.a2009s/Destrieux.simple.2009-07-29.gcs atlas).

For each anatomical region, the following information is provided: arbitrary index referring to the text, tables and figures of this paper, short name as it appears in the interface window of FreeSurfer, long name and alternative names also found in the literature, terms found in the Terminologia Anatomica are bold typed, inflated view (see fig. 1) on which this label is visible (A: anterior, I: inferior, L: lateral, M: medial, P: posterior, S: superior), boundary corrected concordance index (CIC), and average area (cm²) for right (Rh) and left (Lh) hemispheres. To limit the influence of possible manual labeling inconsistency on the values of areas provided here, we included individual values obtained from the manual and automated (jack-knifing) procedure for each subject. No statistical comparison was provided given the small size of the sample and the large number of parcellations.

Table 2

Area, global CI and percentage of hidden cortex across 12 subjects.

	Right Hemisphere			Left Hemisphere		
	Total	Core	Boundaries	Total	Core	Boundaries
Area (cm²): average	1015.88	861.26	154.62	1015.89	860.58	155.31
Area (cm²): SD	85.90	76.24	12.85	79.86	69.81	13.97
% of area	100.00%	84.78%	15.22%	100.00%	84.71%	15.29%
% of hidden cortex	55.86%			55.07%		
Concordance index	CI_O	CI_C		CI_O	CI_C	
average for hemisphere	0.79	0.84	0.54	0.80	0.85	0.54
SD for hemisphere	0.022	0.024	0.017	0.016	0.017	0.013

Hemispheric values (average and Standard Deviation, SD) are provided for the Training set (see method) without considering non cortical parcellation (Medial_wall label): area, percentage of hidden cortex (sulcal and sulco-gyral cortex of the lateral fossa), and for concordance index without (CI$_O$) and after boundary correction (CI$_C$). Values for boundaries alone are also provided for comparison. To limit the influence of possible manual labeling inconsistency on the provided values, we included data obtained from manual and automated (jack-knifing) labelling for each subject.